

Effects of chain stiffness and salt concentration on responses of polyelectrolyte brushes under external electric field

Qianqian Cao,^{a)} Chuncheng Zuo, Lujuan Li,^{a)} and Guang Yan

College of Mechanical Science and Engineering, Jilin University, Changchun 130022, China

(Received 25 October 2011; accepted 5 December 2011; published online 21 December 2011)

We report a molecular dynamics study on non-equilibrium dynamics of polyelectrolyte brushes under external electric fields. In this work, the effects of chain stiffness and salt concentration on static and dynamic responses of the brushes are addressed in detail. Our simulations indicate that varying these parameters induce rich electro-responsive behavior of the brushes. The increase of salt concentration results in the enhancement of an opposite electric field formed by non-equilibrium distribution of cations and anions, which resists stretching or shrinkage of grafted chains. At strong positive electric fields, the flexible brushes are more sensitive to the change of salt concentration. When reversing the electric field, the stiff brushes undergo a conformational transition from collapse to complete stretching. At high salt concentrations, dynamic responsive magnitude of the brush thickness to added electric field is strongly reduced. It was found that the fall time for the stiff brush becomes much shorter than that for the flexible brush. Additionally, increasing ion concentration leads to an excess extension or shrinkage of flexible brushes. For strongly stiff brushes, such phenomenon occurs in the presence or absence of salt.

© 2011 American Institute of Physics. [doi:[10.1063/1.3672190](https://doi.org/10.1063/1.3672190)]

I. INTRODUCTION

The scientists experimentally have constructed a rich variety of artificial nanochannels, which is attracting widespread interest because their potential applications in biosensors, drug delivery, nanofluidic devices, etc.^{1,2} For example, biomimetic smart nanochannels can be used as a basic platform to simulate the process of ionic transport in living organisms and boost the development of bioinspired smart apparatus.² Smart nanochannels can respond to ambient stimuli such as pH, temperature, light, electric potential, ions, and molecules for regulating ionic transport properties. With the development and application of nanofluidics, nanochannels become key building blocks for the construction of lab-on-a-chip devices which provide useful research tools for ion transport, bionanotechnology, investigation of single-molecular behavior, and biochemical analysis. Moreover, improving smart regulation of nanochannels has become one challenging topic for lab-on-a-chip developments. Almost certainly, surface modification is a very important way to implement the functions of smart nanochannels. In all surface modification technologies, an extensively adopted surface modification approach is grafting polymer chains onto the surface of channels.

When charged polymer chains are grafted densely on a substrate surface, also known as polyelectrolyte brushes, the brushes will exhibit rich conformational behavior due to the long-range electrostatic interaction between charged particles. The conformations of polyelectrolyte brushes depend on many factors, such as salt concentration, grafting density, pH, and charge fraction of polyelectrolyte chains. To deeply understand these systems,

^{a)}Authors to whom correspondence should be addressed. Electronic addresses: qqcao07@mails.jlu.edu.cn and llj09@mails.jlu.edu.cn.

a considerable number of theoretical studies have been performed by means of different methods, including self-consistent field theories,^{3,4} scaling laws,^{5–7} and molecular theories.⁸ Several reviews have been published, summarizing the progress on polyelectrolyte brushes.^{9–12} Experimentally, the integration of stimuli responsive polyelectrolyte brushes into solid-state single nanochannels can create tailor-made nanovalves resembling the functions of sophisticated biological ion channels.¹³ The gating mechanism is implemented by collapse-stretching conformational transition of the brushes responsive to pH. Additionally, coating amphoteric molecules (lysine or histidine) onto the inner surface of an asymmetric nanometer-scaled channel permits a broad set of rectification properties and enables a higher degree of ion transport regulation.¹⁴ More recently, Hou *et al.* developed a pH gating ionic transport nanodevice using plasma asymmetric chemical modification with various complicated functional molecules coated onto the wall of single nanochannels to enhance the functionality of biological ion channels.¹⁵

The natural presence of charges in polyelectrolyte brush systems provides the possibility of using external electric fields to regulate their conformations. Moreover, the electric field represents a favorite approach to induce extension-collapse transition of polyelectrolyte brushes due to its faster construction than other stimuli. Recent studies indicated that polyelectrolyte brushes can respond to the change of applied electric field normal to the grafting surface.¹⁶ Our group has studied the electroosmosis transport in a nanochannel grafted with polyelectrolytes under the control of an electric field normal to the channel wall using molecular dynamics simulations.¹⁷ Under the effects of added electric fields, the coupling of polyelectrolyte chain dynamics and electrohydrodynamics leads to some new electrokinetic transport phenomena. Ouyang *et al.* have also reported molecular dynamics simulations of the gating behaviors of polyelectrolyte brushes in a nanochannel under external electric field.¹⁸ Their results indicated that pressure-driven flow can be well controlled through switching on and off external electric fields, because varying electric field can induce extension/collapse transition of the polyelectrolyte brushes. Experiments by Weir *et al.* based on weak polybase brushes showed that voltage-induced swelling exhibits a wider range of brush swelling states in comparison to pH switching.¹⁹ Moreover, the additional advantages of the voltage stimulus are shown to be remotely controlled and may be fully automated.

The salt concentration as a variable parameter can tune the conformational behavior and dynamics of polyelectrolytes. Many experimental and theoretical works have been devoted to address the scaling relationship between salt concentration and conformational transition of single brushes^{8,20–23} as well as the effects of salt concentration on interactions between apposing brushes.^{24–26} Recently, some research groups have paid particular attention to interactions between two rigid polyelectrolyte brushes, such as the dependence between distance and force as well as interaction mechanisms.^{27–29} It was found that unlike flexible polyelectrolyte brushes, the force between stiff brushes not only arises from the osmotic stress of compressed counterions within the brush but also from the work required to bend the rigid chains.²⁷ We have also investigated the self-assembly of surfactants and bottle-brush polyelectrolytes with varying backbone stiffness,³⁰ and the conformational behavior of grafted bottle-brush polyelectrolytes with stiff side chains³¹ and flexible ones.³² Our results demonstrated that the change of backbone stiffness leads to different aggregate morphologies.³⁰ Wynveen and Likos have explored the combined effects of salt concentration and chain stiffness on the interactions between two polyelectrolyte brushes.²⁸ They suggested that bending-force contribution also depends on the ionic environment within the brush due to reduced effective persistence length of the chains induced by ionic screening. Here, we carry out molecular dynamics simulations to address the effects of chain stiffness and salt concentration on non-equilibrium conformational behavior of polyelectrolyte brushes under external electric field. Note that Ouyang *et al.* have analyzed static and dynamic behavior of partially charged brushes in response to electric fields.¹⁶ The present work extends their study to account for the addition of salt and chain stiffnesses, and further explore new responsive characteristics of polyelectrolyte brushes. The rest of the paper is organized as follows: In Sec. II, we introduce the model system followed by the details of molecular dynamics simulations. Following

that, we present simulation results and a detailed discussion of the results. Conclusions are summarized in Sec. IV.

II. MODEL AND SIMULATION METHOD

We use molecular dynamics simulations to investigate the effects of chain stiffness and salt concentration on conformational behavior of polyelectrolyte brushes in the presence of external electric field. The chains are modeled using a widely utilized, coarse-grained bead spring model. We take σ , m , and ε_{LJ} as length, mass, and energy units, respectively. All other units are derived from these basic units, such as time unit $\tau = (m\sigma^2/\varepsilon_{LJ})^{1/2}$, temperature unit $T^* = \varepsilon_{LJ}/k_B$ (k_B is Boltzmann constant), and electric field unit $E^* = \varepsilon_{LJ}\sigma^{-1}/(4\pi\varepsilon_0\sigma\varepsilon_{LJ})^{1/2}$ (ε_0 is the vacuum permittivity). In the brush systems, one end of polyelectrolyte chains with $N = 30$ monomers is fixed and arranged in a square lattice with a spacing $d = \rho_g^{-1/2}$, where ρ_g denotes the number of end-grafted chains per unit area. In present work, a fixed grafting density, $\rho_g = 0.0625\sigma^{-2}$, is taken. Every two monomer of the chain carries a negative charge. Grafted monomers can be viewed as ghost particles that are fixed and do not interact with other particles. The salt concentration c as a variable parameter changes in a range from 0 to $0.08\sigma^{-3}$. In the presence of salt ions, the cations in the bulk fluid include the counterions dissociated from polyelectrolytes and the dissociated salt cations. The dimensions of the simulation box are $N_x d \times N_y d \times L_z$, where $N_x = N_y = 8$, $L_z = 40\sigma$. Periodic boundary conditions are applied in the x - and y -directions. We exert an electric field E perpendicular to the channel wall to control the extension rate of polyelectrolyte brushes.

The short-range interaction between any two particles is modeled by a purely repulsive Lennard-Jones (LJ) potential. The chain's connectivity is maintained by a finitely extendable nonlinear elastic (FENE) potential with the maximum bond length $R_0 = 1.5\sigma$ and the spring constant $k_b = 30\varepsilon_{LJ}/\sigma^2$. This choice of parameters gives an average bond length $a = 0.98\sigma$. We take into account the bending rigidity of the backbone through using a harmonic angle potential. A fully flexible backbone is mimicked by setting $k_\theta = 0$, and $k_\theta = 450k_\theta^*$ corresponds to a strong chain stiffness where $k_\theta^* = \varepsilon_{LJ}/\text{rad}^2$ is the unit of chain stiffness. Electrostatic interactions are calculated using the particle-particle/particle-mesh (PPPM) algorithm.³³ To calculate the Coulomb interaction of the systems with a slab geometry which is periodic in the x - and y -directions and have a finite length in the z -direction, an empty volume with the height of $3L_z$ is inserted along the z -direction. Additionally, a correction term is also added to the modified PPPM method.³⁴ The system temperature is controlled by a Langevin thermostat based on the fluctuation-dissipation theorem.³⁵ In addition to the temperature control, the effects of solvent molecules (water) are also taken into account implicitly through frictional and random forces in Langevin dynamics. The damping rate γ and the desired temperature T are set to $1.0\tau^{-1}$ and $1.2T^*$. In this work, we choose $\sigma = \lambda_B$ where $\lambda_B = e^2/(4\pi\varepsilon_0\varepsilon_r k_B T)$ is the Bjerrum length and ε_r denotes the dielectric constant of the solvent, respectively. The Bjerrum length for water is 0.71nm at room temperature (300K), so that σ is also approximately 0.71nm. Therefore, the highest salt concentration studied is $c = 0.37\text{ mol L}^{-1}$ ($0.08\sigma^{-3}$). We take the dielectric constant as $\varepsilon_r = 80$ to reproduce some properties of water. Further, at $T = 300\text{ K}$ the value of electric field unit E^* is about 0.294 V/nm , and the unit of chain stiffness $k_\theta^* = 2.078\text{ kJ mol}^{-1}\text{ rad}^{-2}$ is obtained. For grafted chains with $k_\theta = 0$, our model can be viewed as a coarse-grained representation of flexible polyelectrolytes such as poly(sodium styrenesulfonate) (NaPSS) and ssDNA. Stiff dsDNA chains were modeled with $k_\theta = 360k_\theta^*$ at low ionic strength. However, dsDNA bending energy constant is affected by the salt concentration. Our simulations correspond to a range of chain stiffness from $k_\theta = 0$ to $935\text{ kJ mol}^{-1}\text{ rad}^{-2}$ ($k_\theta = 450k_\theta^*$), which can cover polyelectrolyte chains with various stiffnesses in real systems. The positions and velocities of the particles are solved using the velocity-Verlet algorithm with a time step $\Delta t = 0.005\tau$. More details on the model potentials used in the paper have been described by Ouyang *et al.*¹⁶ and our group.^{17,31} Initially, cations and anions are randomly dispersed within the simulation box. Polyelectrolyte chains stretch normal to the grafting surface. Figure 1 gives a simulation snapshot of the initial model system. The system is equilibrated for 1.5×10^5 time

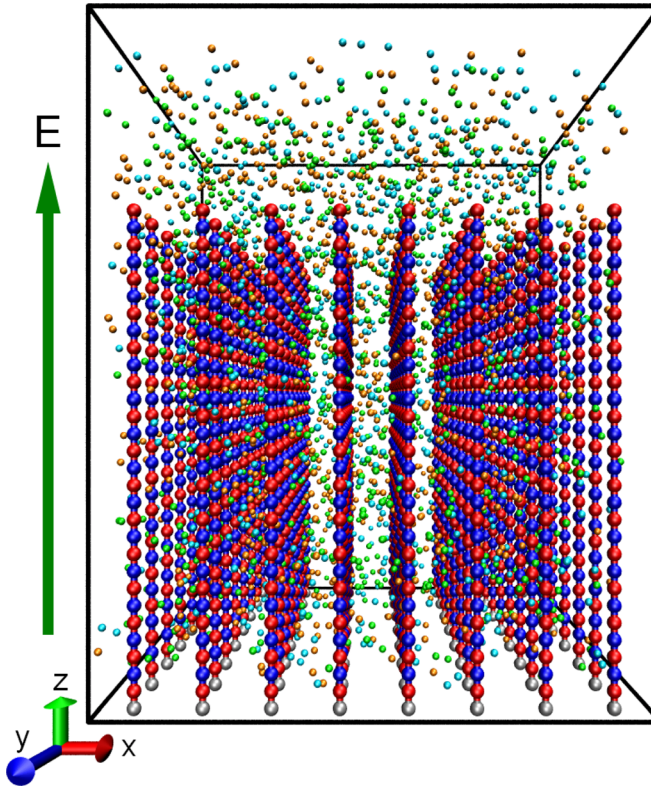


FIG. 1. Snapshot of the initial model system. Grafted chains are in an extended state. An electric field E is applied normal to the wall to control the stretching/shrinkage of the polyelectrolyte brush. Red and blue beads represent charged and neutral monomers, respectively. Cations and anions dissociated from salt are shown in orange and cyan, respectively. Counterions from polyelectrolytes are represented as green beads. Grafted monomers are shown in grey.

steps, and then an electric field is added through a further run of 2.5×10^5 time steps. After achieving a steady state, a production run of 4×10^5 time steps is performed to sample the simulation data. In this work, molecular dynamics simulations on non-equilibrium dynamics of polyelectrolyte brushes under external electric fields are carried out using the open-source software LAMMPS.³⁶

III. RESULTS AND DISCUSSION

We first present monomer density profiles $\rho_m(z)$ as a function of the distance from the grafting surface for fully flexible brushes $k_\theta/k_\theta^* = 0$ and strong stiff brushes $k_\theta/k_\theta^* = 450$ at two electric field strengths ($E/E^* = 2$ and -2) and various salt concentrations. As shown in Figure 2, the chains are in a strong extended state at $E/E^* = 2$. When the direction of electric field is reversed, namely, $E/E^* = -2$, the brush undergoes a collapsed transition (Figure 3). It is found that at $E/E^* = 2$, increasing the salt concentration induces a shift of monomer density profiles towards the grafting surface, that is, chain stretching is reduced with the increase of salt concentration. However, at $E/E^* = -2$, the increase of salt concentration results in a stretching of the brush. One can note that at $E/E^* = 2$, the shrinkage of the flexible brush is more obvious upon growing the salt concentration compared to the stiff brush, while at the opposite electric field $E/E^* = -2$, the stiff brush becomes more sensitive to salt concentrations investigated here (Figure 3(b)). In the absence of salt ions, grafted chains are almost completely collapsed onto the surface, even for the stiff brush (Figure 3(b)). At $c\sigma^3 = 0.03$ and $E/E^* = -2$, though most monomers of the stiff brush aggregate near the grafting surface, there exists a long tail in the density profile. This indicates that a small part of grafted stiff chains extend far towards the bare surface. It should be emphasized that the stiff chains which are

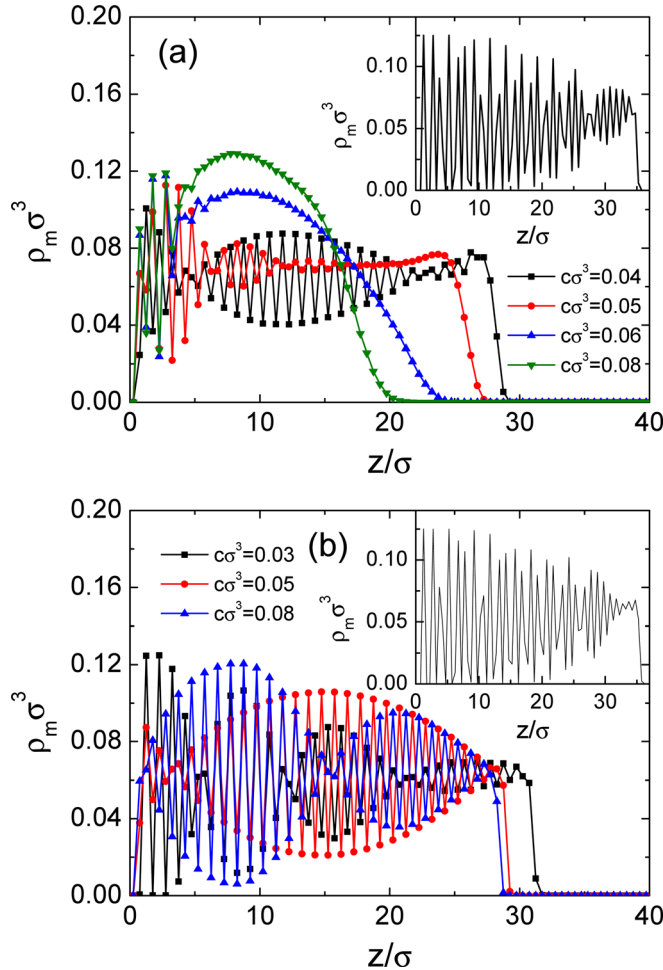


FIG. 2. Density profiles $\rho_m(z)$ of monomers from: (a) flexible polyelectrolyte brushes and (b) stiff polyelectrolyte ones with chain stiffness $k_\theta/k'_\theta = 450$ at different salt concentrations. The insets show monomer density in the absence of salt. Simulation data are obtained at $E/E^* = 2.0$.

collapsed onto the surface still exhibit an extended conformation. However, a long tail of density profiles is not observed for the flexible brush at various salt concentrations (Figure 3(a)). Therefore, there does not occur such phenomenon that only a part of flexible chains extend far towards the bare surface. From the studies of flexible brushes without added electric field (see Figure 5 in Ref. 20), we note that the monomer density profiles are less affected by salt concentration compared to our results at $E/E^* = 2$ (Figure 2(a)). A further discussion on the effect of salt concentration on the brush conformation will be made below.

At $E/E^* = 2$, the density profiles of flexible brush show strong oscillation at $c\sigma^3 = 0.04$ (Figure 2(a)). Moreover, the density oscillation becomes stronger in the absence of salt (the inset of Figure 2(a)). At high salt concentrations, such as $c\sigma^3 = 0.06$ and 0.08 , the monomer densities of flexible brushes can be described through a Gaussian-terminated parabolic volume fraction profile. If not otherwise stated, we refer to density oscillation away from the wall (typically, $z > 2.5\sigma$). The oscillation near the wall is due to the initial segment of the chain starting from the grafting site being perpendicular to the surface. This corresponds to liquid-like behavior near a solid surface. For the stiff brush, strong density oscillation can be observed at various salt concentrations (Figure 2(b)). Note that the shape of oscillation depends on the salt concentration. The oscillation behavior represents a strong extended and ordered brush conformation. At the negative electric field $E/E^* = -2$, the density profile for the stiff brush exhibits a strong oscillation at $c\sigma^3 = 0.08$ (Figure 3(b)), while the density oscillation disappears for the flexible

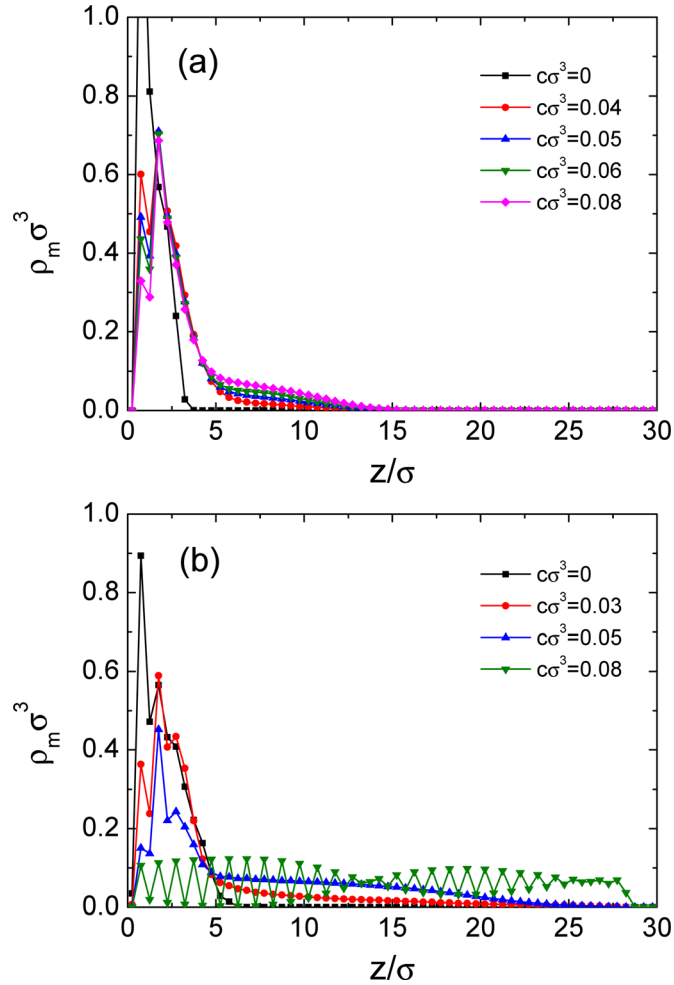


FIG. 3. Density profiles $\rho_m(z)$ of monomers from: (a) flexible polyelectrolyte brushes and (b) stiff polyelectrolyte ones with chain stiffness $k_\theta/k_\theta^* = 450$ at different salt concentrations. Simulation data are obtained at $E/E^* = -2.0$.

brush (Figure 3(a)). In cases without added salt, the density profile of flexible brush shows a similar strong oscillation behavior as that of stiff brush at $E/E^* = 2$ (see the insets in Figure 2). Thus, the flexible chains have enhanced effective stiffness under strong positive electric fields, representing a feature of rigid chain.

We give simulation snapshots of brush systems at different electric fields and salt concentrations in Figure 4. One can obtain a visual picture of conformational transition of the brushes. In this representation, the connectivity of the chains is preserved. This may lead to some chains extend beyond the periodic boundary. For simplicity, we do not assign counterions to the closest chain monomer outside the simulation box. Most counterions distribute freely in the inside of the brush for cases without added salt and electric field, only a small amount of counterions move outside the brush (Figures 4(a) and 4(e)). Some works have reported the details of counterion distribution in polyelectrolyte brushes without added electric fields.^{37,38} Here, we do not make a further discussion on equilibrium distribution of counterions. As discussed above, at $E/E^* = 2$ and $c\sigma^3 = 0.03$, the flexible brush is in a strongly extended state (Figure 4(b)). Obviously, cations aggregate compactly near the top wall, and anions diffuse near the bottom wall. When the electric field is reversed, a collapsed brush conformation is observed (Figure 4(c)). One can note that unlike the cases of positive electric fields, though a significant amount of ions are pulled towards the surfaces, some ions still fill the entire region between two surfaces. Additionally, we further show the density profiles of cations $\rho_c(z)$ and anions $\rho_a(z)$ at $E/E^* = -2$ and $c\sigma^3 = 0.03$ (Figure 5(a)). As seen from the figure, there are indeed a high

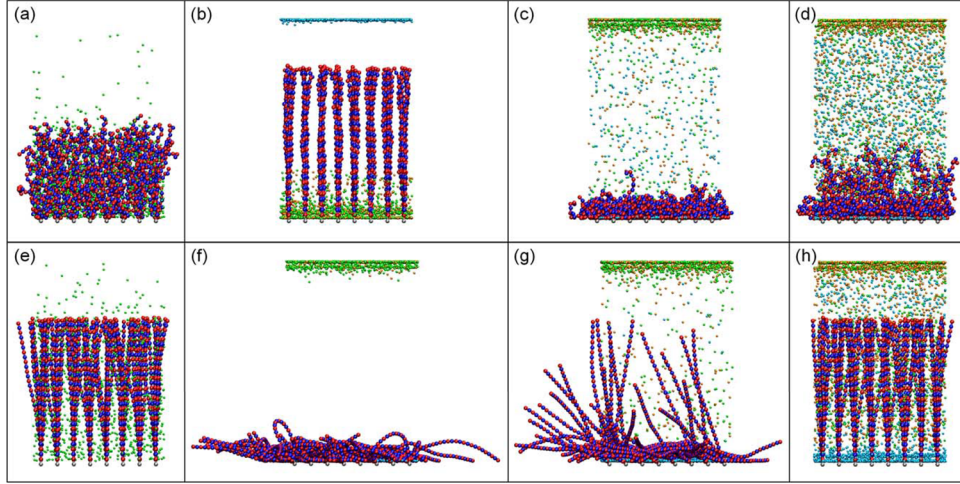


FIG. 4. Typical snapshots of the brush system at different salt concentrations and electric fields. (a)-(d) correspond to flexible brushes: (a) $E/E^* = 0$ and $c\sigma^3 = 0$; (b) $E/E^* = 2.0$ and $c\sigma^3 = 0.03$; (c) $E/E^* = -2.0$ and $c\sigma^3 = 0.03$; (d) $E/E^* = -2$ and $c\sigma^3 = 0.08$. (e)-(h) correspond to stiff brushes with chain stiffness $k_\theta/k_\theta^* = 450$; (e) $E/E^* = 0$ and $c\sigma^3 = 0$; (f) $E/E^* = -2.0$ and $c\sigma^3 = 0.01$; (g) $E/E^* = -2.0$ and $c\sigma^3 = 0.03$; (h) $E/E^* = -2.0$ and $c\sigma^3 = 0.08$.

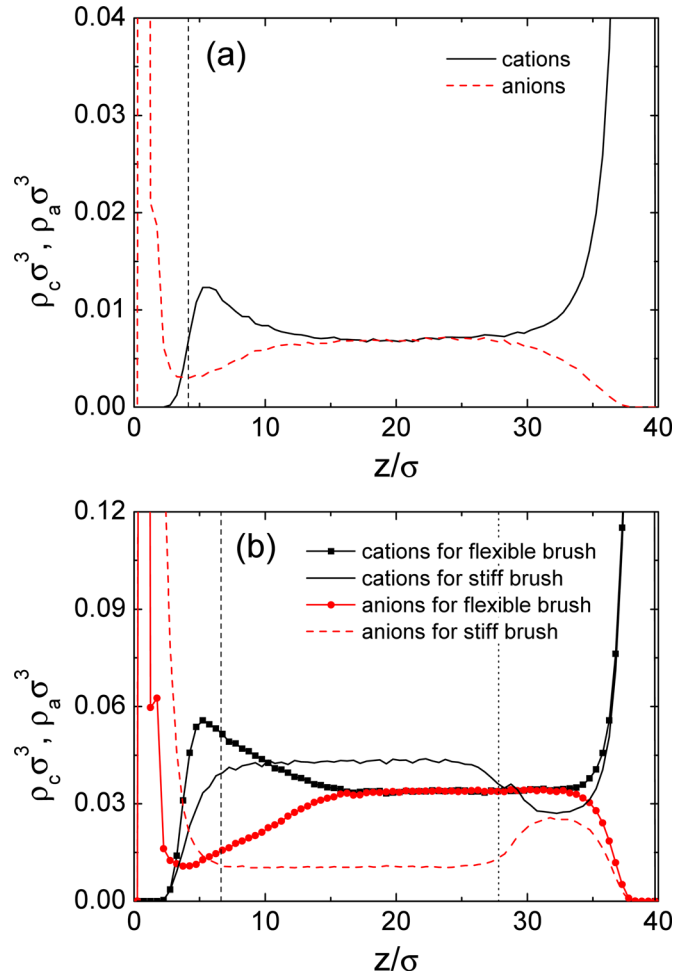


FIG. 5. Density profiles of cations $\rho_c(z)$ and anions $\rho_a(z)$ for: (a) the flexible brush at $c\sigma^3 = 0.03$ and (b) the flexible brush and the stiff one with chain stiffness $k_\theta/k_\theta^* = 450$ at $c\sigma^3 = 0.08$. Simulation data are obtained at $E/E^* = -2.0$.

aggregate amount of ions near the surfaces. Cations and anions reach an equilibrium state in the middle region. The density peak of cations and the density valley of anions near the brush thickness (vertical dashed line in Figure 5(a)) are a result of electrostatic interactions between ions and charged monomers forming a compact polyelectrolyte layer. For the stiff brush, there are a part of the chains which do not collapse on the grafting surface (Figure 4(g)). This is in accordance with the long tail in the density profile of monomers (Figure 3(b)). When decreasing salt concentration to $c\sigma^3 = 0.01$, a full collapse of the stiff brush occurs (Figure 4(f)).

At $E/E^* = -2$ and $c\sigma^3 = 0.08$, the simulation snapshots show that all stiff chains are in an extended state normal to the grafting surface (Figure 4(h)). Moreover, the flexible brush also has a certain amount of swelling (Figure 4(d)) compared to that at a low salt concentration $c\sigma^3 = 0.03$ (Figure 4(c)). Together with the density profile of monomers, the flexible brush should undergo a partial swelling when increasing salt concentration $c\sigma^3 = 0.03$ to 0.08, because the monomer density is apparently lower when $z > 5\sigma$ (Figure 3(a)) and Figure 4(d) also shows a part of polymer chains with a greater degree of stretching. For the case of the high salt concentration, we give the density profiles of cations and anions for the flexible and stiff brushes (Figure 5(b)). It is clear that there are a significant aggregate amount of ions near the surfaces. The number of anions is approximately equal to that of cations in region away from the brush and the bare surface, particularly for the flexible brush, indicating that charge

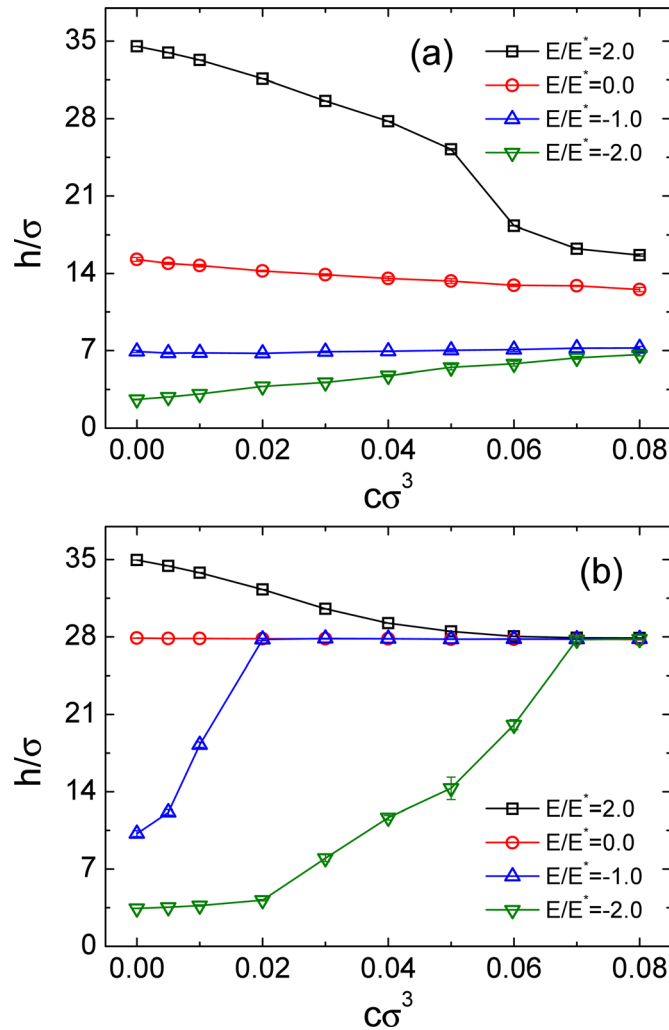


FIG. 6. Average thickness h of: (a) flexible brushes and (b) stiff ones with chain stiffness $k_\theta/k_\theta^* = 450$ as a function of salt concentration at different electric fields.

neutrality is well satisfied. The densities of cations and anions remain constant in a wide region ($8\sigma < z < 25\sigma$) within the stiff brush. Moreover, the differences of charges between anions and cations are balanced out by charged monomers. Further, this also implies an ordered conformation of the stiff brush. We have calculated the local net charge along the direction normal to the surface at high salt concentrations ($c\sigma^3 > 0.04$), namely, $\langle \rho_p \rangle - \langle \rho_n \rangle$, where $\langle \rho_p \rangle$ and $\langle \rho_n \rangle$ denote positive and negative charge density, respectively (the results are not shown here). It is found that the net charge density satisfies a good local approximation away from the surfaces. However, a high non-zero net charge near the surfaces, which induces an excess electric field to resist the added electric field, is observed at strong electric fields.

To investigate quantitatively the extension or shrinkage of the brush, we calculate the average thickness of the grafted layer using the formula $h = \left\langle \left[\sum_{i=1}^{N_g} z_i^{\max} \right] / N_g \right\rangle$, where z_i^{\max} is the maximum value of z -coordinates of the monomers from the i th polymer chain, and $N_g = N_x \times N_y$ denotes the number of grafted polyelectrolyte chains. Figure 6 gives the brush thickness h as a function of the salt concentration for fully flexible brushes and stiff ones with $k_\theta/k_\theta^* = 450$. At strong electric fields, such as $E/E^* = 2.0$ and -2.0 , the thickness of the flexible brush shows a sensitive response on the salt concentration (Figure 6(a)). The effect of salt concentration becomes slight when weakening the electric field. At $E/E^* = 2.0$, the brush thickness decreases with increasing the salt concentration. In contrast, an increase of the brush thickness is observed at $E/E^* = -2.0$. If the electric field is removed, the brush is found to shrink upon increasing the salt concentration, which is consistent with computational works on polyelectrolyte brushes with added salt.²⁰ Moreover, this behavior is in agreement with some experimental results.^{19,23} The behavior of the brush corresponds to a nonlinear osmotic regime. For the stiff brush, its thickness scarcely changes with the salt concentration in the absence of electric field (Figure 6(b)). This indicates that reduced osmotic pressure of counterions due to Debye screening effects is not enough to overcome bending energy of stiff chains. One can note that the stiff brushes in the presence of electric fields reach the same thickness as that without electric field at high salt concentrations. The aggregation of cations and anions near the surfaces leads to the form of an electric field in opposite direction to the external electric field. The increase of salt concentration can enhance the opposite electric field, which resists significantly stretching or contraction of polyelectrolyte chains. Therefore, the stiff brushes under different electric fields tend to achieve a similar conformational state with increasing salt concentration. The suppression effect on chain stretching or contraction is also observed for the flexible brushes. At $E/E^* = 2.0$, the stiff brush exhibits a relatively small extension at low salt concentrations compared to that at $E/E^* = -2.0$. This is because the stiff brush in the equilibrium state already adopts a strongly extended conformation. Enhancing positive electric field

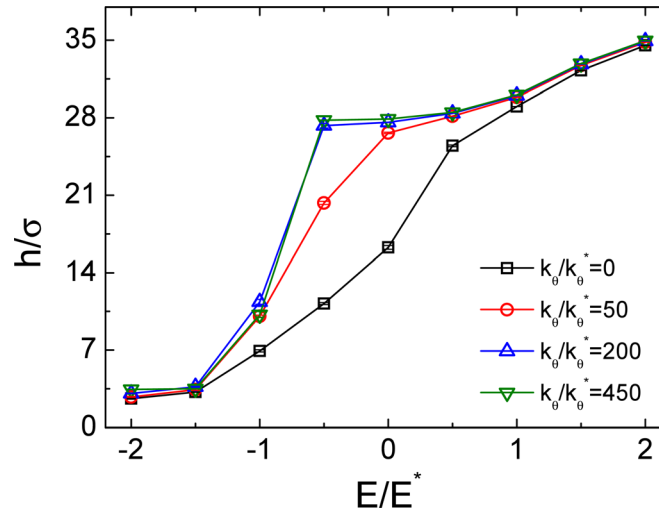


FIG. 7. Average thickness h of the brush as a function of electric field at different chain stiffness.

has a weak influence on the chain stretching. Oppositely, the stiff brush undergoes a collapsed conformational transition at an enhanced negative electric field.

In the absence of added salt, the effect of varying electric field and chain stiffness on the brush thickness is also investigated. We present the brush thickness as a function of electric field at different chain stiffness in Figure 7. Clearly, enhancing the electric field leads to an increase of the brush thickness. As observed experimentally,¹⁹ PDMAEMA

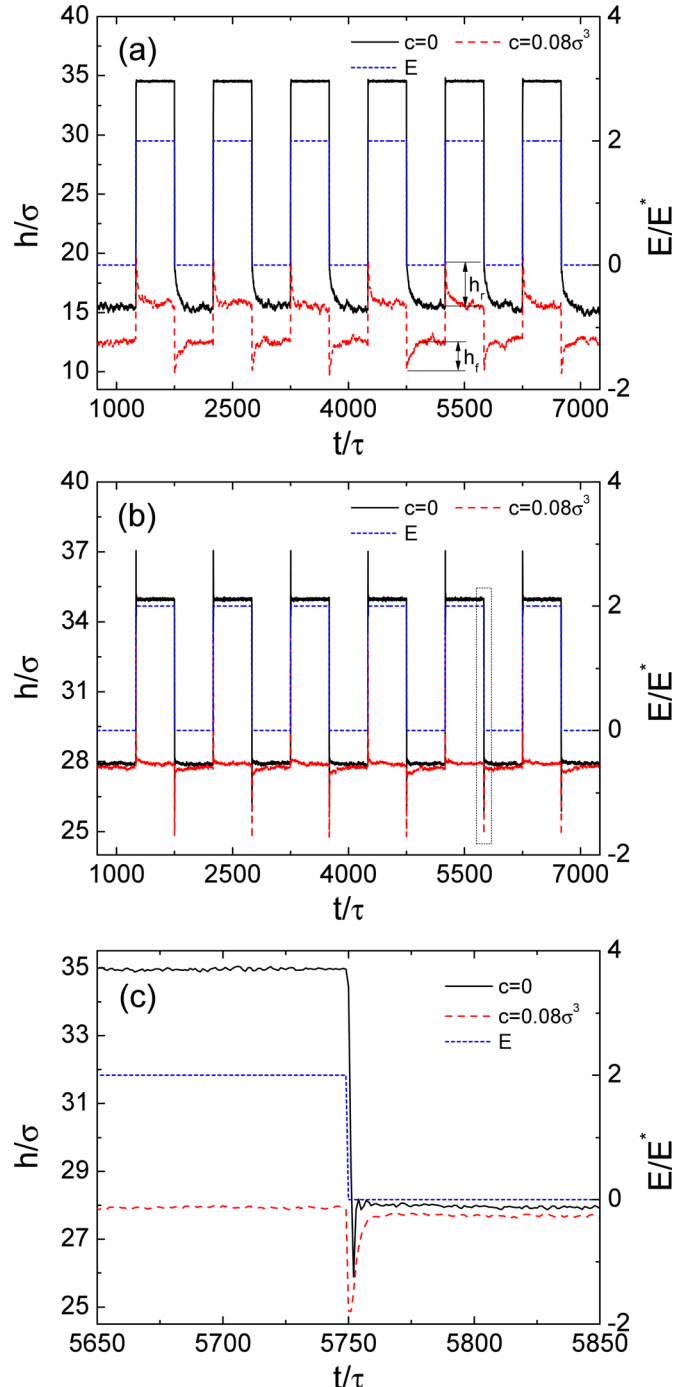


FIG. 8. Dynamic response of brush thickness h under an alternate square-wave electric field for: (a) flexible brushes and (b) stiff ones with chain stiffness $k_\theta/k_\theta^* = 450$, in the absence of salt and at $c\sigma^3 = 0.08$. (c) zooms on the dashed region in (b).

(poly(2-(dimethylamino)ethyl methacrylate)) brushes under positive electric fields exhibit a swelling state, while they undergo a collapse transition for cases of negative electric fields. At strong electric fields, the brush thickness has a relatively small difference for the brushes with different chain stiffness. However, at weak electric fields, $-1.0 < E/E^* < 0.5$, the chain stiffness can affect significantly the brush thickness. It reveals that in a range of weak electric fields, the bending energy of polymer chains is comparable with external interaction exerted by the electric field on charged monomers and internal electrostatic correlation between charged ions. In cases of strong chain stiffness studied, such as $k_\theta/k_\theta^* = 200$ and 450 , the change of brush thickness with electric field obeys a similar relationship. It is also found that the brush stretches rapidly away from the grafting surface when $E/E^* > -1.5$ up to a certain value of electric field depending on chain stiffness (such as -0.5 for $k_\theta/k_\theta^* = 200$ and 450).

We also investigate dynamic responsive behavior of polyelectrolyte brushes under an alternate square-wave electric field. Accordingly, an electric field of $E/E^* = 2.0$ is added and removed alternatively. The frequency of alternative electric field is fixed at $0.001\tau^{-1}$. The simulation results are obtained in the absence of salt and at the highest salt concentration studied $c = 0.08\sigma^3$ for fully flexible brush and highly stiff brush with stiffness $k_\theta/k_\theta^* = 450$. Before the alternative electric field is applied, we first run an equilibrium simulation for 2.5×10^5 time steps. As shown in Figures 8(a) and 8(b), the responsive magnitude is significantly reduced at $c = 0.08\sigma^3$. In particular, the thickness almost remains constant for the stiff brush (Figure 8(b)). In the absence of salt, compared to the stiff brush there is a larger responsive magnitude for the flexible brush (about 19σ , only 7σ for the stiff brush). For the flexible brush without salt ions, the dynamic behavior of the brush is similar to that reported by Ouyang and co-workers.¹⁶ Obviously, the fall time, which the brush returns to the equilibrium state when the electric field is removed, becomes much shorter for the stiff brush (90τ without salt) than for the flexible brush (260τ without salt).

It is noteworthy that in the presence of salt, the flexible brush exhibits a sudden extension h_r (when the electric field is added) and an abrupt shrinkage h_f (when the electric field is removed) followed by a stable brush thickness (Figure 8(a)), which is not observed for the non-salt case. A similar phenomenon also occurs for the stiff brush regardless of the presence or absence of salt (Figure 8(b)). For the cases with salt, the average excess extension \bar{h}_r and the average excess shrinkage \bar{h}_f of the stiff brush are 5.8σ and 3.1σ , respectively, which are larger than those in the absence of salt ions ($\bar{h}_r \approx \bar{h}_f \approx 2.1\sigma$). Therefore, increasing the ion concentration leads to a stronger excess extension or shrinkage. Figure 8(c) shows a local detail of dashed region in Figure 8(b). The excess change of brush thickness disappears within a short time. The sudden change of the brush thickness is caused by non-equilibrium motion of chains and ions. When the brush is in a strongest extended state, the ions still do not reach a stable distribution. Then, the chains begin to shrink until the stable distribution of the ions is achieved.

IV. CONCLUSIONS

Molecular dynamics simulations have been performed to investigate conformational transition and dynamic response of polyelectrolyte brushes under added electric fields. We address the effects of salt concentration and chain stiffness as variable parameters. In the absence of electric field, the flexible brushes are found to shrink with increasing salt concentration, but the highly stiff brushes hardly change their thickness in the range of salt concentrations studied here. It reveals that the decrease of counterion osmotic pressure due to Debye screening effects is not enough to overcome bending energy of stiff chains. The presence of externally applied electric field leads to a rearrangement of positively and negatively charged ions. At strong electric fields, a significant amount of anions and cations move towards two different surfaces. This non-equilibrium ion distributions further result in the form of an internal electric field in the direction opposite to external electric field, which resists stretching or shrinkage of grafted chains induced by external electric field. The internal electric field becomes stronger at higher salt concentrations, because more ions aggregate near the surfaces. It needs to be noted that though there is a high net charge near the surfaces, electroneutrality conditions away from the

surfaces are satisfied at the local scale. At strong electric fields, the flexible and stiff brushes exhibit different sensitivity in response to varying salt concentration. For example, at a strong positive electric field ($E/E^* = 2.0$), the flexible brushes are more sensitive to salt concentration, and density profiles of their monomers undergo a transition from high oscillations to Gaussian-terminated parabola shape. When the electric field is reversed, the stiff brushes can change their conformations from collapse to full stretching. Finally, we analyzed the dynamic responsive behavior of polyelectrolyte brushes. In the same ion environment, the stiff brushes show a weaker responsive magnitude to the electric field due to high intrinsic chain stiffness. Additionally, an excess extension or shrinkage is observed for stiff brushes as well as flexible brushes at high salt concentrations. This is caused by the inconsistency between the establishment of equilibrium distribution of small ions and dynamic response of polyelectrolyte chains under external electric fields. Polyelectrolyte brushes as potential components for soft nanotechnology will play an important role to implement the smart valve in nanofluidics technology.

ACKNOWLEDGMENTS

This work was supported by the National Natural Science Foundation of China (Nos. 30770501 and 51175223).

- ¹T. M. Fyles, *Chem. Soc. Rev.* **36**, 335 (2007).
- ²X. Hou, W. Guo, and L. Jiang, *Chem. Soc. Rev.* **40**, 2385 (2011).
- ³E. B. Zhulina and O. V. Borisov, *J. Chem. Phys.* **107**, 5952 (1997).
- ⁴O. V. Borisov, F. A. M. Leermakers, G. J. Fleer, and E. B. Zhulina, *J. Chem. Phys.* **114**, 7700 (2001).
- ⁵P. Pincus, *Macromolecules* **24**, 2912 (1991).
- ⁶F. S. Csajka, R. R. Netz, C. Seidel, and J. F. Joanny, *Eur. Phys. J. E* **4**, 505 (2001).
- ⁷P. M. Biesheuvel, *J. Colloid Interface Sci.* **275**, 97 (2004).
- ⁸P. Gong, J. Genzer, and I. Szleifer, *Phys. Rev. Lett.* **98**, 018302 (2007).
- ⁹J. Rühe, M. Ballauff, M. Biesalski, P. Dziezok, F. Grohn, D. Johannsmann, N. Houbenov, N. Hugenberg, R. Konradi, S. Minko, M. Motornov, R. R. Netz, M. Schmidt, C. Seidel, M. Stamm, T. Stephan, D. Usov, and H. N. Zhang, *Adv. Polym. Sci.* **165**, 79 (2004).
- ¹⁰M. Ballauff and O. Borisov, *Curr. Opin. Colloid Interface Sci.* **11**, 316 (2006).
- ¹¹F. Zhou and W. T. S. Huck, *Phys. Chem. Chem. Phys.* **8**, 3815 (2006).
- ¹²R. Barbey, L. Lavanant, D. Paripovic, N. Schuwer, C. Sugnaux, S. Tugulu, and H. A. Klok, *Chem. Rev.* **109**, 5437 (2009).
- ¹³B. Yameen, M. Ali, R. Neumann, W. Ensinger, W. Knoll, and O. Azzaroni, *Nano Lett.* **9**, 2788 (2009).
- ¹⁴M. Ali, P. Ramirez, S. Mafe, R. Neumann, and W. Ensinger, *ACS Nano* **3**, 603 (2009).
- ¹⁵X. Hou, Y. J. Liu, H. Dong, F. Yang, L. Li, and L. Jiang, *Adv. Mater.* **22**, 2440 (2010).
- ¹⁶H. Ouyang, Z. H. Xia, and J. Zhe, *Nanotechnology* **20**, 195703 (2009).
- ¹⁷Q. Q. Cao, C. C. Zuo, L. J. Li, and Y. H. Zhang, *Microfluid. Nanofluid.* (2011).
- ¹⁸H. Ouyang, Z. H. Xia, and J. Zhe, *Microfluid. Nanofluid.* **9**, 915 (2010).
- ¹⁹M. P. Weir, S. Y. Heriot, S. J. Martin, A. J. Parnell, S. A. Holt, J. R. P. Webster, and R. A. L. Jones, *Langmuir* **27**, 11000 (2011).
- ²⁰N. A. Kumar and C. Seidel, *Macromolecules* **38**, 9341 (2005).
- ²¹T. Wu, P. Gong, I. Szleifer, P. Vlcek, V. Subr, and J. Genzer, *Macromolecules* **40**, 8756 (2007).
- ²²R. Nap, P. Gong, and I. Szleifer, *J. Polym. Sci., Part B: Polym. Phys.* **44**, 2638 (2006).
- ²³Y. Mei and M. Ballauff, *Eur. Phys. J. E* **16**, 341 (2005).
- ²⁴F. Kremer, M. M. Elmahdy, A. Synytska, A. Drechsler, C. Gutsche, P. Uhlmann, and M. Stamm, *Macromolecules* **42**, 9096 (2009).
- ²⁵S. Block and C. A. Helm, *Phys. Rev. E* **76**, 030801 (2007).
- ²⁶S. Hayashi, T. Abe, N. Higashi, M. Niwa, and K. Kurihara, *Langmuir* **18**, 3932 (2002).
- ²⁷A. Wynveen and C. N. Likos, *Phys. Rev. E* **80**, 010801 (2009).
- ²⁸A. Wynveen and C. N. Likos, *Soft Matter* **6**, 163 (2010).
- ²⁹K. Kegler, M. Salomo, and F. Kremer, *Phys. Rev. Lett.* **98**, 058304 (2007).
- ³⁰Q. Q. Cao, C. C. Zuo, L. J. Li, and H. W. He, *Soft Matter* **7**, 6522 (2011).
- ³¹Q. Q. Cao, C. C. Zuo, and L. J. Li, *Eur. Phys. J. E* **32**, 1 (2010).
- ³²Q. Q. Cao, C. C. Zuo, Y. H. Ma, L. J. Li, S. Y. Chen, and Z. Y. Hu, *J. Polym. Sci., Part B: Polym. Phys.* **49**, 882 (2011).
- ³³R. W. Hockney and J. W. Eastwood, *Computer Simulation Using Particles* (Adam Hilger, Bristol, 1988).
- ³⁴I. C. Yeh and M. L. Berkowitz, *J. Chem. Phys.* **111**, 3155 (1999).
- ³⁵G. S. Grest and K. Kremer, *Phys. Rev. A* **33**, 3628 (1986).
- ³⁶S. Plimpton, *J. Comput. Phys.* **117**, 1 (1995).
- ³⁷F. S. Csajka and C. Seidel, *Macromolecules* **33**, 2728 (2000).
- ³⁸Q. Q. Cao, C. C. Zuo, H. W. He, and L. J. Li, *Macromol. Theory Simul.* **18**, 441 (2009).